ChemComm

Check for updates

Photoswitchable inhibitors: temporally regulated inhibition of the IDO1 enzyme using photoactive merocyanine derivatives

Niku Moni Das,[a] Sayantani Biswas,[b] Suravi Chauhan,[c] Adyasa Sahoo,[a] Debdas Dhabal [ID][a] and Debasis Manna [ID] *[ab]

Developing photoactive molecules represents an emerging strategy for temporally regulated inhibition of the indoleamine 2,3-dioxygenase 1 (IDO1) enzyme. Interestingly, only the photoactive merocyanine isomer of a potent compound effectively binds to both the apo-IDO1 protein and heme cofactor, enabling photoisomer-specific enzyme inhibition. These phototunable molecules hold significant promise for advancing targeted immunotheranostics.

Immunotherapy is an innovative approach to combat cancer and Alzheimer's disease by rejuvenating the immune system to target and eliminate disease-causing cells or pathological markers. In cancer immunotherapy, immune checkpoint inhibitors rejuvenate antitumor immunity by obstructing the 'off' signals from immune checkpoint proteins, thereby allowing T cells to target and destroy cancer cells effectively.[1–3] In Alzheimer's disease, immunomodulation focuses on neuroinflammatory processes and abnormal protein deposits, such as amyloid-beta and tau, to slow the progression of the disease.[2] Cytokine (such as IFN-γ, TNF-α)-mediated overexpression of the indoleamine 2,3-dioxygenase 1 (IDO1) enzyme under pathogenic conditions leads to the uncontrolled metabolism of L-tryptophan (L-Trp), which significantly contributes to immune suppression, tumour growth, neurodegeneration, and other pathological processes.[4] Therefore, IDO1 is a promising target for combating cancer, Alzheimer's disease, and other pathological conditions.

In the last decade, various inhibitors, including indoximod, linrodostat, and epacadostat, have been developed to inhibit the hemin-containing IDO1 enzyme selectively.[5] However, these conventional IDO1 enzyme inhibitors often cause systemic effects that result in widespread immune suppression, potentially leading to adverse side effects and reduced therapeutic benefits. In addition, conventional IDO1 enzyme inhibitors lack the ability to target IDO1 specifically in tissues where its role is most adverse, such as tumours or areas of inflammation.[6] This lack of tissue specificity and the systemic effects might have contributed to the failure of the ECHO-301 Phase III clinical trials, which tested the combination of the IDO1 inhibitor epacadostat with the anti-PD-1 antibody Keytruda for treating metastatic melanoma.[6,7] Recently, inhibitors targeting apo-IDO1 have been developed as an alternative strategy to overcome the limitations of conventional IDO1 inhibitors and to achieve more sustained and potent inhibition.[8–11] These findings indicate that a targeted and dynamic approach to IDO1 inhibition is necessary to enhance the precision and efficacy of treatment.

The use of photoswitchable compounds presents a promising approach in addressing the challenges of targeted IDO1 inhibition, as it allows for temporal control, potentially enhancing therapeutic benefits while minimizing systemic side effects.[12,13] Spiropyrans are known to undergo reversible isomerization when exposed to light, transitioning between the ring-closed spiropyran (SP) and ring-opened merocyanine (MC) form, which makes them useful in applications such as chemical sensors, drug delivery systems, and smart materials.[14,15] We hypothesize that the appropriately substituted MC form could selectively bind and inhibit IDO1 in the targeted tissues, only after photoirradiation (Fig. 1A). This strategy could allow us to control the formation of the active inhibitor in a temporal manner and regulate IDO1 activity in the targeted cells and tissues.

Inspired by the benefits of photopharmacology in drug discovery, we designed and synthesized a series of spiropyran derivatives from N-alkylated 2,3,3-trimethylindolenine derivatives.[12,13] The cyclocondensation of N-alkylated 2,3,3-trimethylindolenine with substituted 2-hydroxy benzaldehyde or 2-hydroxy-1-napthaldehyde under basic conditions provided the targeted spiropyran derivatives **2a–2e** and **3a-3e** (Scheme S1). Spectral studies of **3e** demonstrated photo-responsive ($\lambda_{ex} = 400$ nm) isomerization, transitioning from the closed-ring spiropyran to the open-ring

[a] *Indian Institute of Technology Guwahati, Chemistry, Guwahati, Assam, India. E-mail: dmanna@iitg.ac.in*

[b] *Indian Institute of Technology Guwahati, Biosciences and Bioengineering, Guwahati, Assam, India*

[c] *Indian Institute of Technology Guwahati, Center for the Environment, Guwahati, Assam, India*
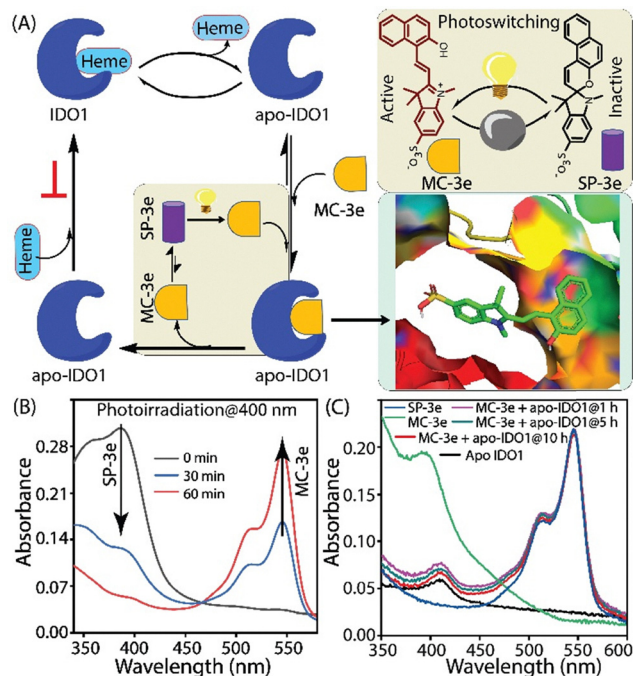
Fig. 1 (A) Schematic diagram representing the photoactive **MC-3e**-mediated inhibition of IDO1 enzyme activity *via* apo-IDO1 binding. (B) Absorbance spectra demonstrating the photoinduced conversion of **SP-3e** to **MC-3e**, both before and after visible light treatment (400 nm). (C) Absorbance spectra of **SP-3e**, **MC-3e**, apo-IDO1, and **MC-3e**-bound apo-IDO1 at different time intervals.
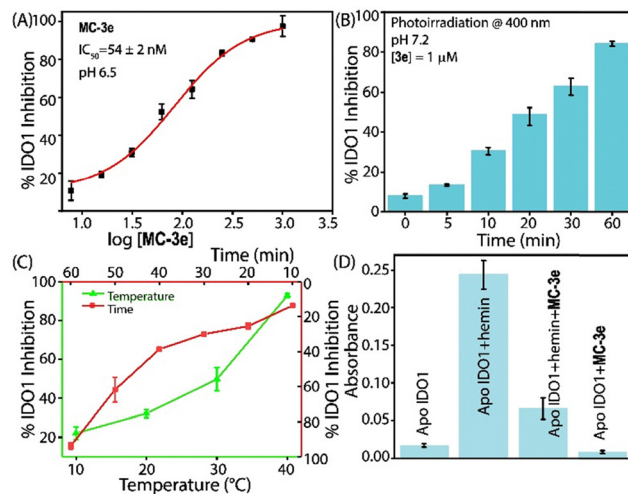

Fig. 2 Inhibitory activities of IDO1 (A) at different concentrations of **MC-3e** at pH 6.5, and (B) after photoirradiation (using LED light) of **MC-3e** with 400 nm light at different time intervals. (C) IDO1 inhibitory activities at different temperatures and time intervals with **MC-3e** at pH 6.5. (D) The activity of apo-IDO1 in the absence and presence of the compound and/or hemin.

Table 1 Inhibitory activity of the spiropyran and merocyanine derivatives against purified human IDO1 enzyme

Compounds	IC$_{50}$ values (nM)	Inhibition (%)	
		0.25 μM	1 μM
MC-3e	54 ± 2	83 ± 1.5	97 ± 1
SP-3e	>10 000	9 ± 1	21 ± 9
Epacadostat pH 6.5	61 ± 6	76 ± 4	96 ± 2

merocyanine isomer and its reversal upon photoirradiation (λ_{ex} = 545 nm) or under dark ambient conditions (Fig. 1B). The spectral studies also revealed the pH-dependent reversible isomerization of **3e** (Fig. S1).[15]

The initial screening of the synthesized compounds using the HPLC-based kynurenine assay revealed that the merocyanine (MC) form of **3e** (**MC-3e**) strongly inhibits the activity of the IDO1 enzyme, with an IC$_{50}$ value of 53.9 ± 2 nM (Fig. 2A, B, Table 1, and Table S2). The **MC-3e** also showed stronger IDO1 inhibitory activity under an acidic environment (Fig. S2). In contrast, the spiropyran derivative isomer of **3e** (**SP-3e**) exhibited significantly weaker IDO1 inhibitory activity (IC$_{50}$ > 10 μM). The other synthesized merocyanine derivatives showed much lower inhibitory activities against IDO1. The potent **MC-3e** exhibited no significant inhibitory activity against the tryptophan 2,3-dioxygenase (TDO) enzyme, which belongs to the same enzyme family as IDO1 (Table S3).

The activity of **MC-3e** encouraged us to explore its detailed inhibitory mechanism on IDO1. A variation in the pre-incubation time period of **MC-3e** with IDO1 enzyme at 37 °C demonstrated a significant increase in its inhibitory activity over time, reaching maximum activity (>90%) at 60 minutes (Fig. 2C). The temperature-dependent activity assays showed that the inhibition of IDO1 by **MC-3e** increased when the temperature was raised from 20 °C to 37 °C. These results indicate that the inhibition process may involve time and temperature-sensitive events, such as the dissociation of the heme cofactor from the IDO1 enzyme

(Fig. 2C). The binding of **MC-3e** to "pocket C", the dynamic JK-loop region (360–380 AA) of the IDO1 enzyme, could induce heme release. The flexibility and plasticity of this loop are crucial for the activity and substrate selectivity of the enzyme.[16,17]

To determine whether the loss of the heme-cofactor is a decisive step in the inhibition process of the IDO1 enzyme, we performed UV-Vis spectroscopic analysis both in the presence and absence of **MC-3e**. The results showed a decrease in the Soret peak in the presence of **MC-3e**, indicating that heme was released from IDO1.[11] Notably, no significant changes were observed in the Soret peaks of TDO or other heme-containing proteins, such as haemoglobin and myoglobin, suggesting that the hemin loss induced by **MC-3e** is selective for the IDO1 enzyme (Fig. S3). For further investigation of the **MC-3e**-mediated release of the heme cofactor from the IDO1 enzyme, a protoporphyrin IX (PPIX)-based fluorescence quenching assay was performed. A significant decrease in the PPIX fluorescence upon the addition of **MC-3e** indicated the interaction between PPIX and hemin. In contrast, no observable change in the PPIX

fluorescence signal was detected in the presence of **SP-3e** (Fig. S4 and S5). Thus, these UV-Vis and fluorescence spectral changes of the IDO1 enzyme and PPIX suggest the potential for **MC-3e**-mediated release of the heme from IDO1. Additionally, we did not observe any significant changes in the circular dichroism (CD) spectra of IDO1 before and after incubation with **MC-3e**, indicating that the compound-mediated release of the heme cofactor from the IDO1 active site is not caused by any significant alteration in its structural integrity (Fig. S6 and Table S4). Therefore, removing the heme-cofactor from the IDO1 enzyme and generating apo-IDO1 are crucial steps in the IDO1 inhibitory activity of **MC-3e**.

A concentration-dependent activity assay was performed to investigate the rate-limiting process of **MC-3e**-mediated IDO1 inhibition. The activity assay was performed after incubating the IDO1 enzyme with **MC-3e** for 60 minutes. The IDO1 activity at various concentrations of **MC-3e** exhibited a non-linear relationship. The IDO1 inhibition assay in the presence of L-Trp and the reducing agents (ascorbate, methylene blue, and catalase) against different concentrations of **MC-3e** also showed a nonlinear inhibition profile, suggesting that the oxidation state of iron does not influence the **MC-3e**-mediated IDO1 inhibitory activity in the hemin group. Therefore, releasing the heme cofactor or generating the apo-IDO1 protein is the rate-limiting step of the **MC-3e**-mediated IDO1 inhibition mechanism. The UV-Vis spectral analysis showed that the extent of reduction of the Soret peak was quite similar for both the catalytically active and inactive IDO1 enzyme, indicating that the release capability of the heme cofactor was nearly the same (Fig. S7). The apo-IDO1 protein equilibrated with external hemin regained its catalytic activity, whereas the apo-IDO1 protein equilibrated with **MC-3e** failed to show any significant activity even after adding external hemin (Fig. 2D).

Recent studies indicate that free hemin is necessary for cellular homeostasis and plays a dual role in cancer, where its accumulation and metabolic dysregulation promote tumour growth by generating oxidative stress and inflammation. However, hemin deficiency also impairs critical cellular functions, necessitating careful regulation of hemin metabolism. Various spectrometric techniques were employed to investigate whether **MC-3e** exhibits hemin-binding properties. The concentration-dependent decrease of the Soret peak indicated that **MC-3e** also interacts with the free heme cofactor. The binding affinities of these **MC-3e** are similar to quinine, a known hemin-binding molecule (Fig. S8). The time-dependent decrease in PPIX fluorescence in the presence of hemin indicates the interaction of PPIX with hemin. However, the addition of **MC-3e**, in combination with hemin, significantly alters the degree of PPIX fluorescence quenching induced by hemin, indicating the potential interaction of **MC-3e** with hemin (Fig. S9). In contrast, the addition of **SP-3e**, in combination with hemin, did not result in any significant alterations in the PPIX fluorescence quenching caused by hemin. Thus, the PPIX-based fluorescence studies indicate that **MC-3e** could inhibit the activity of overproduced labile hemin, whereas **SP-3e** failed to do so. The photo- or pH-induced conversion of **SP-3e** to **MC-3e**, as well as the interaction between **MC-3e** and apo-IDO1, was examined using various
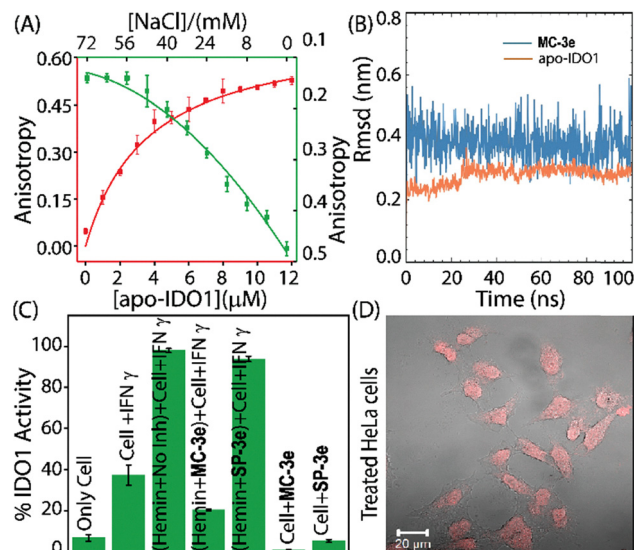

Fig. 3 (A) Steady-state fluorescence anisotropy measurements of **MC-3e** (500 nM) in the presence of various concentrations of apo-IDO1 protein (0–12 μM) and in the absence and presence of different concentrations of NaCl (0–75 mM). (B) The variation in RMSD obtained for apo IDO1 (orange) and **MC-3e** (blue). (C) IDO1 inhibition activity in cells with and without IFN-γ treatment in the presence and absence of the isoforms of **3e**. (D) Confocal microscopy image of **MC-3e**-treated HeLa cells.

spectroscopic methods. The steady-state fluorescence anisotropy measurements of **MC-3e** showed a significant increase in anisotropy with increasing concentrations of apo-IDO1, resulting in a binding affinity (K_d) of 3.9 ± 0.58 μM (Fig. 3A and Fig. S10A).[18] Additionally, the introduction of NaCl led to a concentration-dependent decrease in the steady-state anisotropy value, indicating that the interaction between **MC-3e** and apo-IDO1 is reversible (Fig. 3A and Fig. S10B). The time-dependent UV-Vis spectral studies of **MC-3e** in equilibrium with apo-IDO1 were conducted under neutral and dark conditions. The absorbance profiles of **MC-3e** in the presence of apo-IDO1 exhibited minimal variation over time. This indicates that the **MC-3e** isomer remains stable within the binding site of apo-IDO1 and does not experience significant photochemical or structural changes during a prolonged incubation period of up to 10 h (Fig. 1C and Fig. S11A, B). However, the control study without apo-IDO1 showed that the merocyanine (**MC-3e**) spontaneously converted to the spiropyran isomer (**SP-3e**) under similar experimental conditions (Fig. S11C, D). Hence, these spectral studies suggest a strong and persistent interaction between **MC-3e** and the apo-IDO1, which is crucial for the **MC-3e**-mediated inhibitory activity of IDO1.

To investigate the molecular determinants responsible for the binding of **MC-3e** to the apo-IDO1, molecular docking and molecular dynamics (MD) simulations were performed. The molecular docking analysis of **MC-3e** with the X-ray co-crystal structure of the apo-IDO1 protein (PDB ID: 6AZW) revealed that **MC-3e** is located within the binding pocket of the apo-IDO1 (Fig. S12A).[19] The MD simulation studies (100 ns) showed that **MC-3e** remains strongly bound to the apo-IDO1, with an RMSD of 0.2 nm, while **MC-3e** stabilized at 0.1 nm (Fig. 3B).

The viability assay of **MC-3e** showed low toxicity in HeLa and HEK-293 cells (after 48 h), indicating that this compound is suitable for IDO1 inhibitory studies (Fig. S13). The calculated IC_{50} value for **MC-3e** using the IFN-γ-treated HeLa cells was found to be 5.8 ± 0.7 nM. The cellular IDO1 activity assays demonstrated a considerable increase in IDO1 activity when treated with external IFN-γ and hemin, suggesting that a notable amount of apo-IDO1 is present in the cellular environment. Under similar experimental conditions, hemin, which was equilibrated with the potent compound, demonstrated a significant decrease in IDO1 activity. This suggests that the complexation of hemin with the **MC-3e** hinders the ability of apo-IDO1 to rebind hemin (Fig. 3C and Fig. S14). Therefore, compound binding to the apo-IDO1 and the formation of the hemin-**MC-3e** complex could inhibit the cellular IDO1 activity. The confocal microscopic images revealed distinct red fluorescent puncta in treated HeLa cells, confirming internalization of **MC-3e**, while untreated control cells showed no fluorescence (Fig. 3D and Fig. S16).

The ability to respond to visible light and changes in pH provides a mechanism for the controlled inhibition of the IDO1 enzyme, offering the prospect of targeted therapeutic intervention with minimized off-target effects. The acidic pH-dependent isomerization of **3e** from inactive (**SP-3e**) to active (**MC-3e**) IDO1 enzyme inhibitor offers a significant advantage, because a lower extracellular pH typically characterizes the tumour microenvironment compared to healthy tissues.[20] The visible light can serve as an external stimulus to convert an inactive inhibitor of the IDO1 enzyme into an active one. This approach also offers significant advantages for biomedical applications, as it has relatively low phototoxicity and allows for deeper tissue penetration compared to ultraviolet light.[21] Therefore, the inherent properties of spiropyran derivatives make them a promising scaffold for the development of smart drugs that effectively respond to specific stimuli in a temporally controlled manner, particularly in the field of immunotherapy.

In summary, we synthesized a series of spiropyran derivatives and identified **3e** as a potent and stimuli-responsive inhibitor of IDO1. Upon exposure to light, **3e** undergoes conversion to the photoactive **MC-3e** isoform, which exhibits strong IDO1 inhibitory activity in comparison to that of the photoinactive **SP-3e** isoform. By facilitating the release of heme from holo-IDO1 and transforming it into the apo form, the **MC-3e** exhibits the ability to bind both apo-IDO1 protein and free hemin. These findings highlight a novel strategy for the temporal regulation of IDO1 activity by utilizing light and pH as external stimuli. Compared to traditional IDO1 inhibitors, this photoresponsive approach offers significant potential for the development of temporally regulated therapies for cancer, Alzheimer's disease, and other pathological conditions, enabling greater specificity and safety.

Conflicts of interest

There are no conflicts to declare.

Data availability

The data supporting this article have been included as part of the supplementary information (SI). Supplementary information: detailed experimental procedures, compound characterization, ion transport activity data, and catalytic activity data. See DOI: https://doi.org/10.1039/d5cc05796e.

References

1 A. C. Newman, M. Falcone, A. H. Uribe, T. Zhang, D. Athineos, M. Pietzke, A. Vazquez, K. Blyth and O. D. K. Maddocks, *Mol. Cell*, 2021, **81**, 2290–2302.e2297.

2 P. S. Minhas, J. R. Jones, A. Latif-Hernandez, Y. Sugiura, A. S. Durairaj, Q. Wang, S. D. Mhatre, T. Uenaka, J. Crapser and T. J. S. Conley, *Science*, 2024, **385**, eabm6131.

3 S. Panda, N. Pradhan, S. Chatterjee, S. Morla, A. Saha, A. Roy, S. Kumar, A. Bhattacharyya and D. J. S. R. Manna, *Sci. Rep.*, 2019, **9**, 18455.

4 K. Watcharanurak, L. Zang, M. Nishikawa, K. Yoshinaga, Y. Yamamoto, Y. Takahashi, M. Ando, K. Saito, Y. Watanabe and Y. Takakura, *Gene Ther.*, 2014, **21**, 794–801.

5 R. M. Al-Zoubi, M. Elaarag, A. R. Al-Qudimat, E. A. Al-Hurani, Z. E. Fares, A. Farhan, S. R. Al-Zoubi, A. Khan, A. Agouni, M. Shkoor, H. Bawadi, Z. Z. Zakaria, M. Al Zoubi and K. Alrumaihi, *Front. Pharmacol.*, 2025, **16**, 1632446.

6 K. Tang, Y. H. Wu, Y. H. Song and B. Yu, *J. Hematol. Oncol.*, 2021, **14**, 68.

7 S. Rossini, S. Ambrosino, C. Volpi, M. L. Belladonna, M. T. Pallotta, E. Panfili, C. Suvieri, A. Macchiarulo, G. Mondanelli and C. Orabona, *Front. Immunol.*, 2024, **15**, 1346686.

8 L. Cen, Y. Wu, M. He, J. Huang, W. Ren, B. Liu, L. Meng, L. Huang, H. Gu and Y. Xu, *J. Med. Chem.*, 2025, **68**, 6633–6655.

9 M. T. Nelp, P. A. Kates, J. T. Hunt, J. A. Newitt, A. Balog, D. Maley, X. Zhu, L. Abell, A. Allentoff and R. Borzilleri, *Proc. Natl. Acad. Sci. U. S. A.*, 2018, **115**, 3249–3254.

10 N. M. Das, B. M. Prusty, N. Pradhan, A. Gupta, M. Carmena-Bargueño, R. Karn, H. Pérez-Sánchez, S. Kumar and D. Manna, *Eur. J. Med. Chem. Rep.*, 2023, **9**, 100110.

11 N. Pradhan, N. Akhtar, B. Nath, J. Peña-García, A. Gupta, H. Pérez-Sánchez, S. Kumar and D. J. C. C. Manna, *Chem. Commun.*, 2021, **57**, 395–398.

12 M. J. Fuchter, *J. Med. Chem.*, 2020, **63**, 11436–11447.

13 Y. Liu, T. Wang and W. Wang, *Chem. Soc. Rev.*, 2025, **54**, 5792–5835.

14 C. L. Fleming, S. Li, M. Grøtli and J. Andréasson, *J. Am. Chem. Soc.*, 2018, **140**, 14069–14072.

15 M. Reifarth, M. Bekir, A. M. Bapolisi, E. Titov, F. Nußhardt, J. Nowaczyk, D. Grigoriev, A. Sharma, P. Saalfrank and S. Santer, *Angew. Chem., Int. Ed.*, 2022, **61**, e202114687.

16 K. N. Pham, A. Lewis-Ballester and S. R. Yeh, *J. Am. Chem. Soc.*, 2019, **141**, 18771–18779.

17 U. F. Rohrig, O. Michielin and V. Zoete, *J. Med. Chem.*, 2021, **64**, 17690–17705.

18 L. F. Cheow, R. Viswanathan, C. S. Chin, N. Jennifer, R. C. Jones, E. Guccione, S. R. Quake and W. F. Burkholder, *Anal. Chem.*, 2014, **86**, 9901–9908.

19 N. M. Das, B. M. Prusty, A. Sahoo, P. Mazumder, S. Chauhan, G. Hazarika, S. Kumar, D. Dhabal and D. J. R. M. C. Manna, *RSC Med. Chem.*, 2025, **16**, 3240–3250.

20 S. Yamamoto, K. Nishimura, K. Morita, S. Kanemitsu, Y. Nishida, T. Morimoto, T. Aoi, A. Tamura and T. J. B. Maruyama, *Biomacromolecules*, 2021, **22**, 2524–2531.

21 M. Shamsipur, A. Ghavidast and A. Pashabadi, *Acta Pharm. Sin. B*, 2023, **13**, 2844–2876.